ISSN: 2447-3359

REVISTA DE GEOCIÊNCIAS DO NORDESTE

Northeast Geosciences Journal

v. 12, nº 1 (2026)

https://doi.org/10.21680/2447-3359.2026v12n1ID40089

Rock slope stability assessment under natural seismic actions using pseudo-static analysis

Avaliação da estabilidade de taludes rochosos sob ações sísmicas naturais utilizando análise pseudoestática

Danilo José da Silva[1]; Carlos Henrique Arroyo Ortiz[2]; Daniel Silva Jaques[3]

[1] UFOP, PPGEM, Ouro Preto/MG, Brazil. E-mail: danilo.jose@aluno.ufop.edu.br. ORCID: https://orcid.org/0009-0009-3989-6629
[2] UFOP, PPGEM, Ouro Preto/MG, Brazil. E-mail: carroyo@ufop.edu.br. ORCID: https://orcid.org/0000-0002-4182-7827
[3] UFOP, PPGEM, Ouro Preto/MG, Brazil. E-mail: daniel.jaques@ufop.edu.br. ORCID: https://orcid.org/0000-0001-6238-591X

Abstract: In most cases, rock slope stability studies do not incorporate dynamic loading conditions associated with natural seismic activities into their analyses. In this context, this study aims to employ probabilistic natural seismic hazard maps to calculate factors of safety using the limit equilibrium method, considering both the static and pseudo-static states of a slope. The methodology involved obtaining the slope geometry data on-site, mapping the orientation of geological structures, and determining the properties and parameters required for the stability analysis. Furthermore, seismic hazard maps were retrieved, along with the recommended step-by-step procedure for calculating the seismic coefficient. The results indicated that the slope is stable under static conditions regarding the planar discontinuity surface. For the application of the seismic force on the block mass over the planar discontinuity surface, the 2% probability of exceedance resulted in the highest reduction in the factor of safety compared to the static condition, with a 43% decrease compared to the other probabilities. Under all three pseudo-static seismic loading conditions, the factor of safety remained above one, indicating a stable condition. It is concluded that the seismic force influences the increase in the mobilizing shear stress and the reduction in the resistive shear stress of the rock slope, resulting in a decrease in the factor of safety.

Keywords: Slope stability; Seismicity; Factor of safety.

Resumo: Na maioria dos casos, os estudos de estabilidade de taludes rochosos não incorporam nas suas análises as condições de carregamento dinâmico associados às atividades sísmicas naturais. Nesse contexto, o objetivo deste estudo é empregar os mapas probabilísticos de risco sísmico natural para calcular os fatores de segurança, utilizando o método de equilíbrio limite, considerando tanto o estado estático quanto o pseudoestático de um talude. A metodologia adotada envolveu a obtenção dos dados de geometria do talude no local, mapeamento da orientação das estruturas geológicas, bem como a determinação das propriedades e parâmetros necessários para a análise de estabilidade. Além disso, foram levantados os mapas de risco sísmico e do passo a passo recomendado para o cálculo do coeficiente sísmico. Os resultados obtidos indicaram que o talude se encontra estável para a condição estática em relação a superfície descontínua planar. Para aplicação da força sísmica na massa de bloco sobre a superfície descontínua planar os 2% de probabilidade de excedência resultou na maior redução do fator de segurança em relação a condição estática. Com uma diminuição de 43% em comparação com as demais probabilidades. Em todas as três condições de carregamento sísmico pseudoestático, o fator de segurança permaneceu acima de um, indicando uma condição de estabilidade. Conclui-se que a força sísmica exerce influência no aumento da tensão de cisalhamento mobilizadora e na redução da tensão de cisalhamento resistiva do talude rochoso, resultando na diminuição do fator de segurança.

Palavras-chave: Estabilidade de taludes; Sismicidade; Fator de segurança.

Received: 04/05/2025; Accepted: 31/03/2026; Published: 02/06/2026.

1. Introduction

Slopes are classified as surfaces inclined relative to the horizontal, composed of soil masses, rock masses, or a combination of both. These structures are divided into two categories: natural and artificial. Natural slopes form without human intervention and are predominantly found in natural hillsides. On the other hand, artificial slopes are created by human action and include highway and railway cuts, embankments, mining benches, dams, and stockpiles. Given that many slopes are subject to risks of human, material, and environmental losses, they are expected to withstand disturbances caused by internal and external agents. Therefore, it is fundamental to evaluate various risk factors to determine an appropriate factor of safety (Gerscovich, 2016; Wyllie, 2017).

Brazil faces constant risks of mass movements on slopes, especially due to the intense rainfall periods that occur annually in the southeastern region of the country. These movements are responsible for significant human, material, and environmental losses, driving several researchers to conduct slope stability studies. A factor frequently neglected in these studies is the influence of natural seismic activities occurring worldwide. Depending on their intensity, these activities can be classified as tremors (for lower values) or earthquakes (for higher values). In both cases, there is a high risk of triggering mass movements on slopes. Seismic waves propagate through the medium, acting as a force that reduces material strength, which can lead to failure. According to data published by the Brazilian Seismographic Network (RSBR), in 2023 alone, approximately 261 seismic events were recorded across the Brazilian territory. Of these, about 121 occurred in the Northeast region, with the states of Bahia and Ceará leading with approximately 50 and 31 detected events, respectively (Wyllie, 2017; Cimellaro & Marasco, 2018; Brazilian Seismographic Network, 2024).

Petersen *et al*. (2018) published probabilistic natural seismic hazard maps for all of South America. These maps were developed based on an extensive temporal seismicity catalog, earthquake recurrence rate models, event size assessments, fault geometry, and ground motion parameters. The curves presented in these maps represent the peak ground acceleration (PGA) and spectral acceleration (SA) for different exceedance probabilities of natural seismic events at 2%, 10%, and 50% over a 50-year period. These maps aim to provide relevant parameters for engineering design criteria, especially in determining the seismic coefficient required to model material failure. Therefore, this study aims to employ these probabilistic natural seismic hazard maps to calculate factors of safety using the limit equilibrium method, considering both the static and pseudo-static states of a slope. This analysis will be applied to probable failure conditions of a rock slope, taking into account the probability of exceedance of the seismic event.

2. Methodology

O The study was conducted in several stages. Initially, field data collection was performed following the guidelines recommended by Wyllie (2017) to establish the slope geometry. Subsequently, structural mapping was carried out regarding the orientation attitude of the slope and the main discontinuities, based on the recommendations proposed by Silva (2023) for kinematic analyses to obtain the probable slope failure modes. Then, the rock strength was determined based on the methodology proposed by Basu & Aydin (2004) and Aydin & Basu (2005). This methodology evaluates rock hardness through the Schmidt hammer rebound, considering corrections related to the orientation and type of hammer used. Furthermore, the density and uniaxial compressive strength were determined through correlations with the rebound values, following the methodologies suggested by Deere & Miller (1966) and Aydin & Basu (2005).

The GSI (Geological Strength Index) values, material constant, and disturbance factor adopted for the rock mass of the slope, as well as the parameters for the Generalized Hoek-Brown and Mohr-Coulomb criteria, were obtained following the methodologies suggested by Marinos & Hoek (2000) and Hoek et al. (2002). The peak ground accelerations (PGA) and spectral accelerations (SA) were determined from the curves related to the slope coordinates, entered into the probabilistic natural seismic hazard maps published by Petersen et al. (2018). In turn, the calculation of the seismic coefficient followed the methodology presented by Kavazanjian *et al*. (2011). With all the data obtained for the studied slope, stability analyses were performed considering both static and pseudo-static conditions. These analyses are essential to evaluate slope stability using the limit equilibrium method. Figure 1 illustrates a simplified flowchart of the stages adopted to conduct the study.

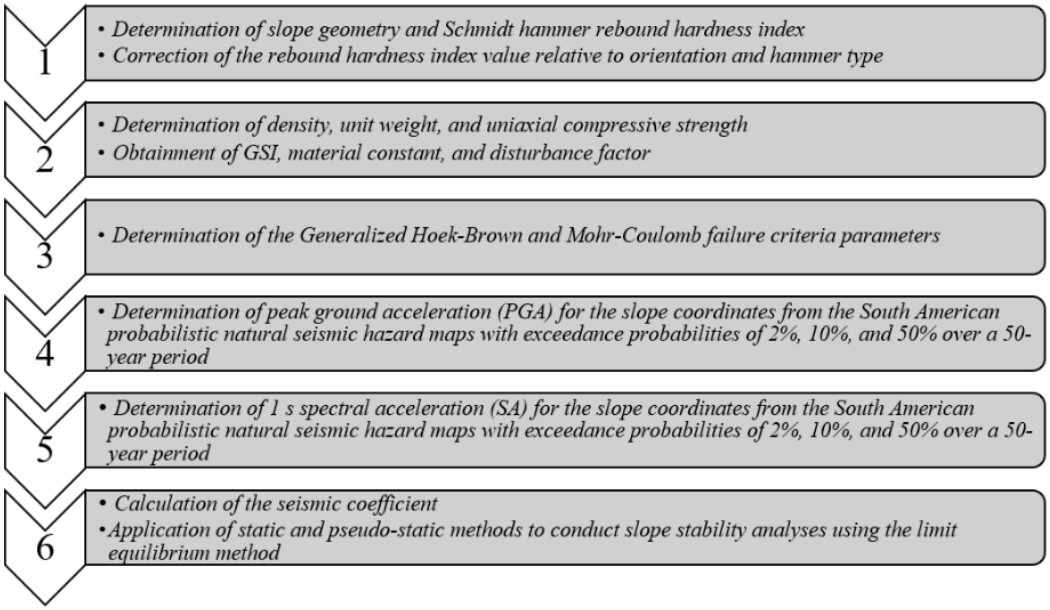

Figure 1 – Simplified flowchart of the stages adopted in the study.
Source: Authors (2024).

3. Results

3.1 Location, geological, and geomechanical description of the slope

The slope targeted in this study (as shown in Figure 2) is located in the municipality of Boa Viagem, in the state of Ceará. It consists of a road cut located on the BR-020 highway, a route with a high traffic volume that represents a geological hazard area due to potential occurrences of mass movements in the rocks. Access to this area is from Fortaleza, also via the BR-020 highway, covering an approximate distance of 254 km. The predominant lithology of the slope is migmatitic gneiss, characterized by complex banding. According to the Geological Survey of Brazil (CPRM) classification, it is a banded orthogneiss presenting schistosity. The slope exhibits multiple discontinuity sets, characterizing it as a jointed rock mass. The predominance of interlocking blocks and the presence of various discontinuities—such as fissures, joints, veins, faults, banding, and schistosity—are relevant characteristics. The orientation attitude of the slope is 300°/87°, which is crucial data for conducting kinematic analyses and identifying potential failure modes based on the orientation of the main discontinuities (Forgiarini *et al*., 2021).

Figure 2 – Slope targeted in the study.
Source: Authors (2024).

3.2 Slope geometry and calculation results of geotechnical properties and parameters

The slope section selected for analysis has an inclination of 87°, with a length from the toe to the crest of the slope of 6.69 m. By establishing a trigonometric relationship between these two metrics to determine the vertical height, an approximate value of 6.68 m is obtained, considering that the slope is practically vertical. The rock rebound measurement was performed directly on the intact portions of the predominant rock present on the slope, at an inclination of +45°. Subsequently, the orientation and the rebound value N were corrected to L, considering the highest 50% of the 20 collected data points. This resulted in an average index value of 49.63. Based on this average rebound, a natural bulk density of 2.51 g/cm³ was determined by correlation, equivalent to a natural apparent unit weight of 24.6 kN/m³. Regarding the uniaxial compressive strength (UCS), which depends on both the rebound value and density, a strength of 120.42 MPa was obtained through correlation. These sequentially calculated data are presented in Table 1.

Table 1 – Calculation results of the geotechnical properties and parameters of the slope.

Property/Parameter	**Data**									
R_N (50% Highest)	61	61	60	60	59	58	54	54	54	53
R_N (+45° for 0°)	62.50	62.50	62	62	61	60	56	56	56	54
R_N for R_L	52.73	52.73	52.26	52.26	51.32	50.38	46.62	46.62	46.62	44.74
Average	49.63									
ρ (g/cm³)	2.51									
γ (KN/m³)	24.60									
UCS (MPa)	120.42									

Source: Authors (2024).

3.3 Parameter results of the Generalized Hoek-Brown and Mohr-Coulomb criteria

For the rock mass of the slope, the structure was classified as Blocky/Disturbed/Seamy, with surface quality ranging from poor to very poor. The GSI was estimated in the range between 15 and 30, with an approximate average value of 23. Considering that the slope has a single predominant rock lithology (gneiss), a single material constant (m_i) was assigned, with an average value of 28. The slope disturbance factor (D) was evaluated based on the blasting condition applied in civil works, resulting in major disturbances to the remaining rock mass. This factor was adopted as 1. The parameters of the Generalized Hoek-Brown and Mohr-Coulomb criteria were obtained using the *RSData* software. Entering the properties and parameters—such as uniaxial compressive strength, GSI, material constant, disturbance factor, natural unit weight, and slope height—allowed for generating the results presented in Figure 3. It is worth noting that the criterion constants and the parameters related to the rock mass are the most relevant in this context.

Hoek Brown Classification	
UCS of intact rock (MPa)	120.42
GSI	23
mi	28
disturbance factor	1
Intact Modulus (MPa)	51540
Hoek Brown Criterion	
mb	0.114
s	2.67e-06
a	0.536

Rock Mass Parameters	
tensile strength (MPa)	0.003
uniaxial compressive strength (MPa)	0.124
global strength (MPa)	4.278
modulus of deformation (MPa)	1256.878
Failure Range Envelope	
application	Slopes
sig3max (MPa)	0.158
Mohr Coulomb Fit	
cohesion (MPa)	0.054
friction angle (°)	47.385

Figure 3 – Results of the geotechnical parameters calculated using the RSData software. Source: Authors (2024).

3.4 Results of the seismic coefficient calculation

Before determining the seismic coefficient (k) for each probabilistic event, it is necessary to obtain several parameters. The PGA and SA for each seismic event were obtained from the probabilistic natural seismic hazard maps for all of South America (Figure 4). These maps contain PGA and SA contours, allowing for the interpolation of these parameter values based on the slope coordinates. These data are extracted using geoprocessing techniques. For each of these parameters, a seismic damping constant related to the material present on the slope is considered. In the case of a medium-hardness rock, the constant was assigned as 0.80 for F_{PGA} and F_y (Kavazanjian *et al*., 2011). With these data, it is possible to calculate the β and α parameters, the latter of which depends on the slope height. Based on all the information obtained, the seismic coefficient was calculated for the exceedance probability of a seismic event over a 50-year period, with probabilities of 2%, 10%, and 50%, respectively. Table 2 presents all the data obtained for these parameters, as well as the results of the seismic coefficients for each evaluated event. It is observed that the 50% probability of exceedance led to the lowest coefficient, since the return period of the event is shorter compared to the 2% exceedance.

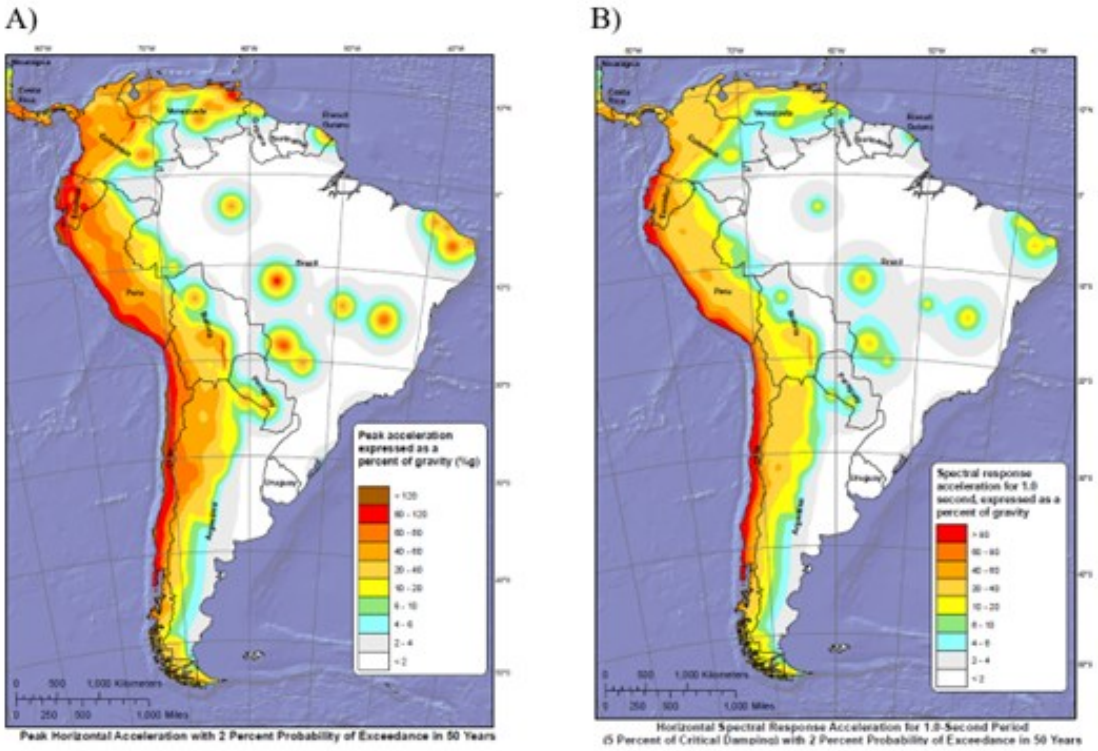

Figure 4 – Probabilistic natural seismic hazard maps for all of South America – A) PGA and B) SA. Source: Authors (2024).

Table 2 – Calculation results of the parameters for obtaining the seismic coefficient.

Parameter	Data		
	2%	**10%**	**50%**
PGA (g)	0,98	0,49	0,20
SA (g)	0,59	0,29	0,10
F_{PGA}	0,80	0,80	0,80
F_V	0,80	0,80	0,80
H (m)	6,68	6,68	6,68
β	0,60	0,59	2
α	0,85	0,84	1
k	0,33	0,16	0,10

Source: Authors (2024).

3.5 Kinematic analysis results

Considering that this is a rock slope, scale is one of the most relevant parameters for classification. Slopes can be categorized as intact rock, jointed rock, or rock mass. Although the studied slope does not have large dimensions, it presents more than four discontinuity sets, which classifies it as a rock mass. Regardless of this classification, it is recommended to conduct kinematic analyses to determine the probable failure modes, taking into account the orientations of the discontinuities. These discontinuities play a fundamental role in the failure conditions of rock slopes. Within the scope of this study, the focus was exclusively on determining the planar failure mode. This is because limit equilibrium analyses can be applied in two dimensions (2D). Wedge failure is addressed with a higher level of detail in three-dimensional (3D) analyses, whereas toppling failure is explored in finite element analyses. The circular approach only applies to highly fractured rocks, where the rock blocks behave as a soil mass.

To perform the kinematic analysis, 10 orientation attitude measurements were collected from the main discontinuities and sets present in the rock mass, as well as the slope orientation. The compass used was calibrated for the magnetic declination of the region, ensuring that the obtained data reflected the true orientation. Based on the friction angle obtained for the rock mass from the correlation envelopes generated by the *RSData* software, the kinematic analysis was conducted using the Dips software. The stereogram configuration adopted included the lower hemisphere, equal-area projection, and a Schmidt stereonet. The planes were represented in the pole format. The kinematic analysis result for the planar failure mode presented in Figure 5 indicates that out of the ten discontinuity and set orientations, only one is in a critical condition for this type of failure. Considering a friction angle of 47°, a slope dip of 87°, a slope dip direction of 300°, and a lateral limit of ±20°, the critical discontinuity has an orientation attitude of 293°/51° and a vertical height relative to the slope toe of 2.35 m. This plane is highly visible in Figure 2, which illustrates the target slope of the study.

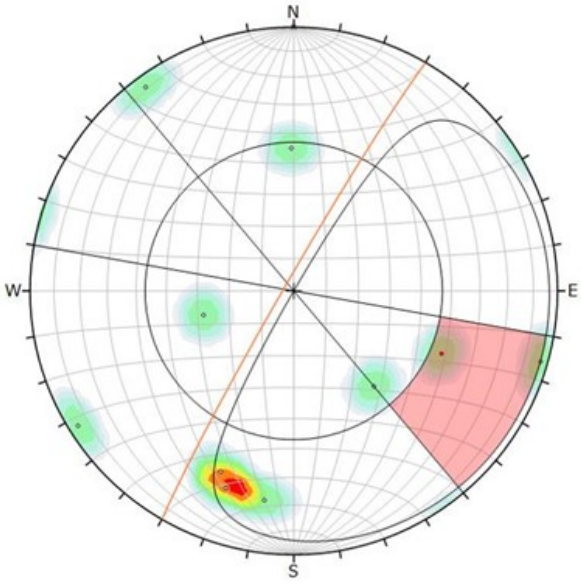

Symbol	Feature
◇	Pole Vectors
◆	Critical Vectors

Color	Density Concentrations
	0.00 - 2.20
	2.20 - 4.40
	4.40 - 6.60
	6.60 - 8.80
	8.80 - 11.00
	11.00 - 13.20
	13.20 - 15.40
	15.40 - 17.60
	17.60 - 19.80
	19.80 - 22.00

Contour Data	Pole Vectors
Maximum Density	21.88%
Contour Distribution	Fisher
Counting Circle Size	1.0%

Kinematic Analysis	Planar Sliding
Slope Dip	87
Slope Dip Direction	300
Friction Angle	47°
Lateral Limits	20°

	Critical	Total	%
Planar Sliding (All)	1	10	10.00%

Plot Mode	Pole Vectors
Vector Count	10 (10 Entries)
Hemisphere	Lower
Projection	Equal Area

Figure 5 – Kinematic analysis results for the planar failure mode.
Source: Authors (2024).

3.6 Factor of safety results under static and pseudo-static conditions for exceedance probabilities of 2%, 10%, and 50% over a 50-year period

Based on the geotechnical properties and parameters, as well as the results obtained from the kinematic analysis, limit equilibrium analyses were performed using the Slide2 software. The 2D slope section modeling considered its height and inclination, thereby establishing an artificial finite representation of the horizontal and vertical extensions within the domain of influence of the problem area. The positioning and orientation of the discontinuity were adopted considering the condition in which it daylighted on the face and crest of the slope. For the failure mode controlled by the discontinuity under planar conditions, Janbu's corrected rigorous slice method was applied for non-circular surfaces. The search for the static and pseudo-static factors of safety was performed using the Block Search configuration. Regarding the total mass of the slope section, the parameters of the Generalized Hoek-Brown failure criterion were employed. For the discontinuity, the parameters of the Mohr-Coulomb criterion were used.

The limit equilibrium analysis result for the rock block mass acting on the planar discontinuity surface yielded a minimum static factor of safety of 2.23. Therefore, this obtained factor indicates that the block mass is highly stable in terms of shear strength along the discontinuity surface, with the magnitude of the strength being more than twice as large

as the mobilizing weight force acting on this potential failure surface. Figure 6 presents the result of this static analysis for the block mass above the planar discontinuity surface.

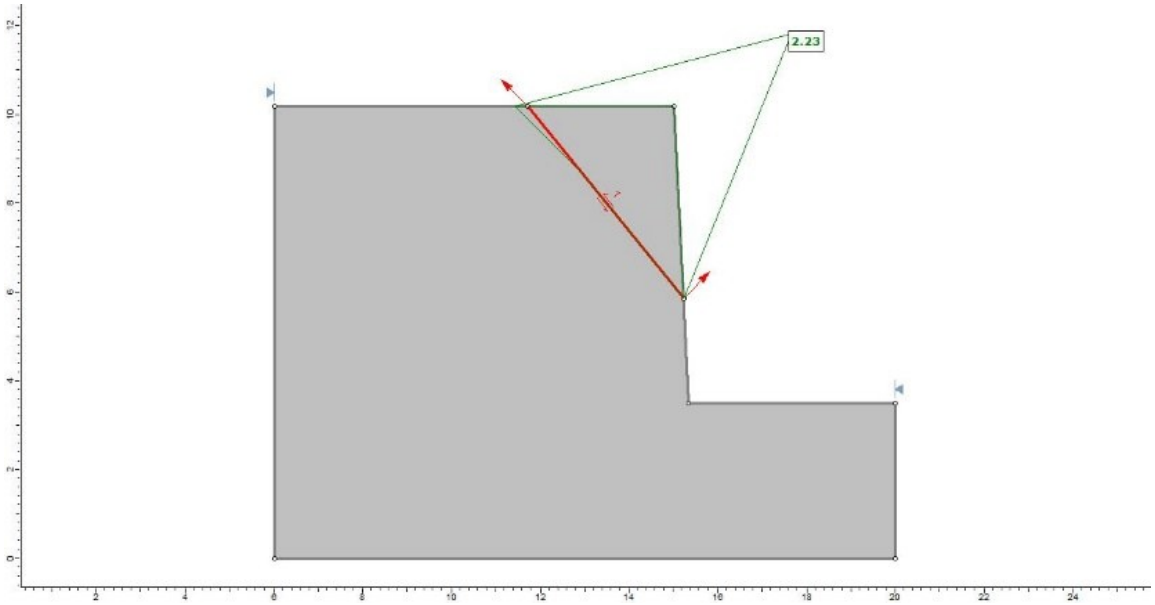

Figure 6 – Static analysis result for the rock block mass above the planar discontinuity surface. Source: Authors (2024).

Using the same data and configurations established for the static factor of safety analysis, in this subsequent evaluation, only the seismic coefficient was introduced as a new parameter to conduct the pseudo-static analysis. Considering an exceedance probability of 2% over a 50-year period, the obtained seismic coefficient was 0.33. Consequently, the pseudo-static factor of safety for the rock block mass acting along the planar discontinuity surface decreased to 1.27, representing a reduction of approximately 43% relative to the static factor of safety, as shown in Figure 7. For the 10% exceedance probability over the same period, the obtained seismic coefficient was 0.16. Under this condition, the pseudo-static factor of safety decreased to 1.72, representing a reduction of about 23% compared to the static factor of safety, as shown in Figure 8. Finally, for the 50% exceedance probability over the 50-year period, the obtained seismic coefficient was 0.10. In this scenario, the pseudo-static factor of safety dropped to 1.90, representing a reduction of approximately 15% compared to the static factor of safety, as shown in Figure 9.

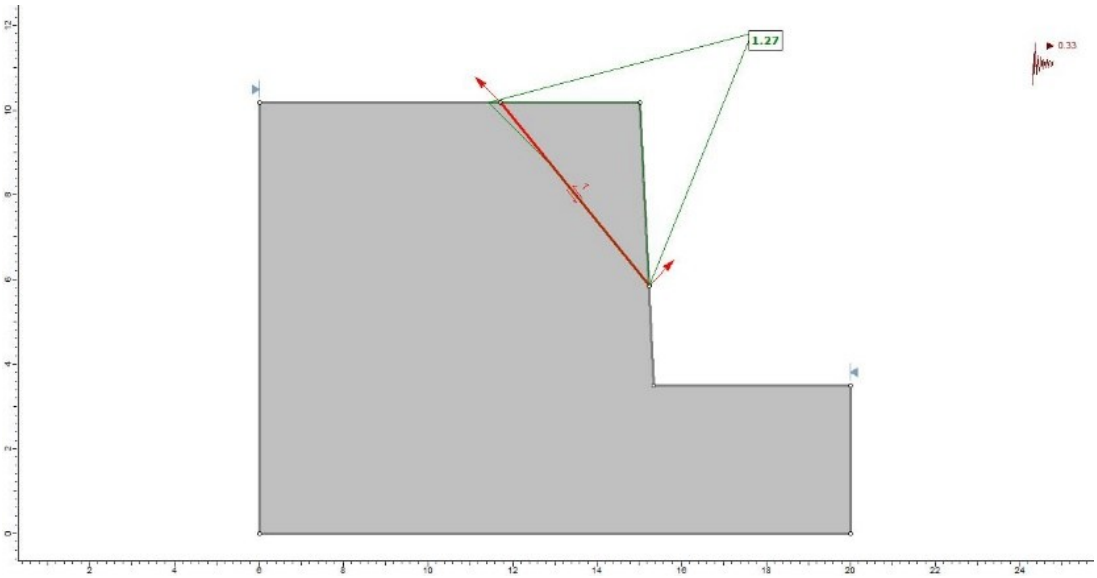

Figure 7 – Pseudo-static analysis result for the rock block mass above the planar discontinuity surface, considering the 2% exceedance probability over a 50-year period.
Source: Authors (2024).

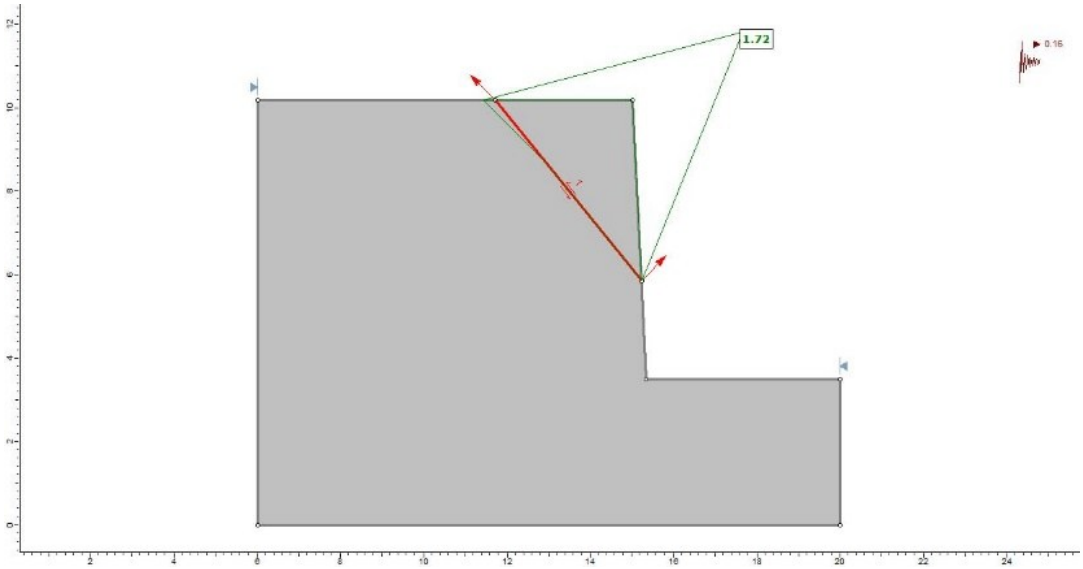

Figure 8 – Pseudo-static analysis result for the rock block mass above the planar discontinuity surface, considering the 10% exceedance probability over a 50-year period.
Source: Authors (2024).

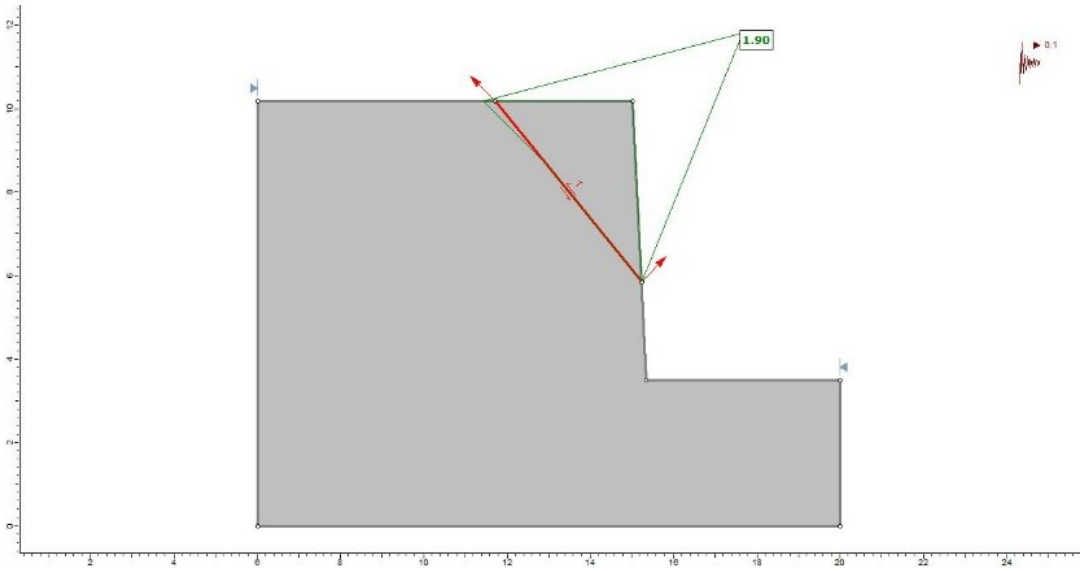

Figure 9 – Pseudo-static analysis result for the rock block mass above the planar discontinuity surface, considering the 50% exceedance probability over a 50-year period.
Source: Authors (2024).

3.7 Discussion

The results obtained in this study clearly demonstrate the significant influence of natural dynamic loads—represented by different levels of seismic exceedance probability—on the stability of rock slopes. It is observed that the analyzed slope presents stable conditions under a static regime, showing a factor of safety of 2.23, which highlights an ample margin of safety in the absence of seismic actions. However, with the introduction of seismic force via the pseudo-static approach, a significant reduction in the factors of safety is verified, especially under the most severe condition (2% exceedance probability over 50 years), where the FS decreases to 1.27, representing a reduction of approximately 43%.

This behavior proves that, even in regions where seismic events are not frequent with large magnitudes, seismic analysis cannot be neglected, especially in fragile geological contexts such as that of the BR-020 highway in Ceará. The classification of the mass as a rock mass, with a significant presence of discontinuities (fissures, joints, banding, and schistosity), suggests that these structures govern the potential instability, particularly in planar failure modes, as identified by the kinematic analysis. Additionally, the seismic coefficients derived from the hazard maps by Petersen et al. (2018) reveal the importance of using regional probabilistic parameters for a more accurate representation of local dynamic loading conditions. This probabilistic approach, which is still seldom applied in geotechnical engineering projects in Brazil, reinforces the importance of incorporating seismotectonic data into the stability analysis process, even for small- to medium-sized projects such as highway slopes.

Another relevant aspect is that, despite the reduction in the factor of safety, the values remained above 1 in all analyses, which, from the perspective of the pseudo-static method, still indicates stability. However, this study points out that the reduction in shear strength can be aggravated by secondary factors, such as heavy rainfall, anthropogenic alterations, or combined seismic events, which could render the structure unstable under more extreme scenarios. Therefore, the obtained results ratify the importance of seismic analysis in slope stability projects, contributing a replicable methodology based on public data (seismic maps and simple field tests like the Schmidt hammer) and widely available tools (RSData, Dips, and Slide2). Furthermore, they reinforce the need for monitoring strategies and preventive planning in zones with historical—even if sparse—seismic records.

4. Conclusion

Based on the exceedance probabilities for a seismic event over a 50-year period, the 2% probability corresponded to the highest peak ground acceleration, spectral acceleration, and seismic coefficient values. As the exceedance probability increases to 10% and 50%, the acceleration and coefficient values decrease. The kinematic analysis for the planar failure

mode indicated only one main discontinuity in a critical condition, with a dip of 51° on the free face of the slope. This discontinuity surface was modeled to perform the analysis, as it directly influences the stability conditions of the rock slope. Furthermore, the limit equilibrium analysis of the block mass acting along the planar discontinuity surface indicated a static factor of safety of 2.23, representing a stable condition.

Regarding the exceedance probabilities, the 2% probability resulted in the largest reduction in the factor of safety, with a 43% decrease compared to the static condition. The 10% probability reduced the factor by 23%, while the 50% probability showed a 15% reduction. Under all three pseudo-static seismic loading conditions, the factor of safety remained above 1, indicating a stable condition for the block mass acting along the planar discontinuity surface. Based on the obtained results, it can be concluded that the seismic force from natural dynamic shocks influences the increase in the mobilizing shear stress and the reduction in the resisting shear stress of the rock slope, resulting in a decrease in the factor of safety. Although the slope in question is classified as a small-scale rock mass, its discontinuity surface still governs the stability conditions. These results highlight the importance of considering the effects of natural or induced dynamic loadings in both slope design and evaluations.

Acknowledgements

This study was financed in part by the Coordenação de Aperfeiçoamento de Pessoal de Nível Superior - Brasil (CAPES) - Finance Code 001. The authors would like to thank CAPES and the Graduate Program in Mineral Engineering at UFOP for their support and funding of this work.

References

Aydin, A.; Basu, A. The Schmidt hammer in rock material characterization. Engineering Geology, v. 81, no. 1, 2005, pp. 1-14.

Basu, A.; Aydin, A. A method for normalization of Schmidt hammer rebound values. International Journal of Rock Mechanics and Mining Sciences, v. 41, no. 7, 2004, pp. 1211-1214.

Cimellaro, G. P.; Marasco, S. Introduction to dynamics of structures and earthquake engineering. 1st ed. Springer International Publishing, Italy, 2018.

Deere, D. U.; Miller, R. P. Engineering classification and index properties for intact rock. National Technical Information Service, Springfield, 1966.

Forgiarini, L. L. et al. Geologia e recursos minerais da folha Independência–SB. 24-V-D-I: Escala 1:100.000: Estado do Ceará [Geology and mineral resources of the Independência sheet–SB. 24-V-D-I: Scale 1:100,000: Ceará State]. CPRM, Fortaleza, 2021.

Gerscovich, D. Estabilidade de taludes [Slope stability]. 2nd ed. Oficina de Textos, São Paulo, 2016.

Hoek, E. et al. Hoek-Brown failure criterion—2002 edition. Proceedings of NARMS-Tac, v. 1, no. 1, 2006, pp. 267-273.

Kavazanjian, E. et al. LRFD seismic analysis and design of transportation geotechnical features and structural foundations. National Highway Institute, Washington, 2011.

Marinos, P.; Hoek, E. GSI: a geologically friendly tool for rock mass strength estimation. ISRM International Symposium, 2000, p. ISRM-IS-2000-035.

Petersen, M. D. et al. Seismic hazard, risk, and design for South America. Bulletin of the Seismological Society of America, v. 108, no. 2, 2018, pp. 781-800.

Rede Sismográfica Brasileira. Boletim sísmico brasileiro [Brazilian seismic bulletin]. Rede Sismográfica Brasileira. Available at: http://rsbr.on.br/pevjs/index.html. Accessed on: March 13, 2024.

Silva, D. J. Diretrizes para a realização de análises de estabilidade de taludes utilizando os métodos de projeção estereográfica e análise cinemática e de sensibilidade [Guidelines for conducting slope stability analyses using

stereographic projection, kinematic, and sensitivity analysis methods]. Revista Brasileira de Geologia de Engenharia e Ambiental, v. 13, no. 1, 2023, pp. 37-55.

Wyllie, D. C. Rock slope engineering. 5th ed. CRC Press, Boca Raton, 2017.